

Triangular Automata: The 256 Elementary Cellular Automata of the Two-Dimensional Plane

Paul Cousin

Université Paris Cité, France

Triangular automata (TA) are cellular automata in the triangular grid. This work focuses on the simplest type of TA, called elementary triangular automata (ETA). They are argued to be the two-dimensional counterpart of Wolfram's elementary cellular automata. Conceptual and computational tools for their study are presented, along with an initial analysis. This paper is accompanied by the author's website, paulcousin.github.io/triangular-automata, where the results can be explored interactively. The source code is available in the form of a Mathematica package at paulcousin.github.io/triangular-automata-mathematica.

Keywords: cellular automata; triangular grid; dynamical systems; complexity

1. Introduction

Cellular automata in the triangular grid (Figure 1), or triangular automata (TA) for short, have already been studied in a few papers [1–17]. This paper will focus on a natural subset of TA called elementary TA (ETA).

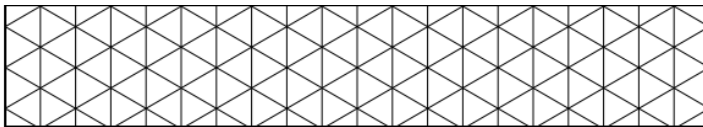




Figure 1. The triangular grid.

ETA cells hold only *binary states*; each cell will thus either be:

- “alive” and colored purple , with a state $s = 1$
- “dead” and colored white , with a state $s = 0$

ETA *rules* determine the future state of a cell based on its current state and the states of its neighbors, regardless of their orientation. This results in only eight possible local configurations, as shown in Figure 2.

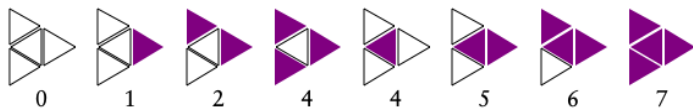


Figure 2. All possible local configurations.

This paper uses a graph-theoretical framework developed in a previous work on graph-rewriting automata [18]. The triangular grid will here be considered as a graph (Figure 3). This graph must be expanded at each time step to simulate an infinite grid. The *region of influence* of a single cell grows in hexagonal layers (Figure 3(a)). This is therefore the most efficient way to expand the graph as well. How to do this in practice is detailed in Section 3.2.

● **Author Query:**
For Figure 3, reduce font size slightly. Is it possible to outline the numbers for (a) in black (the 4 & 5 may be hard to see in print)?

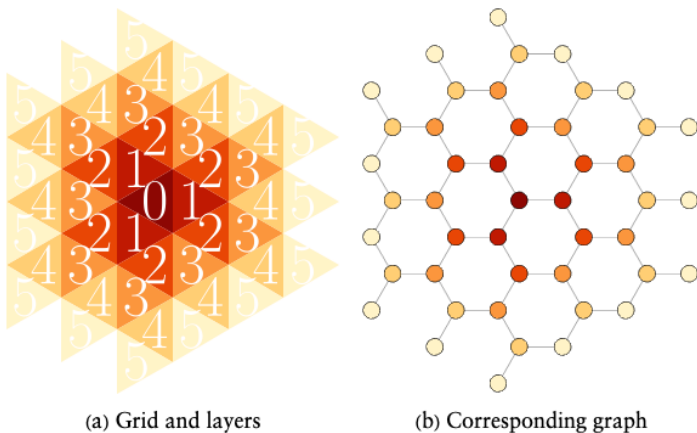


Figure 3. Structure of the triangular grid.

It is useful to see the triangular grid as a graph because computing the evolution of ETA is made quite easy by properties of its *adjacency matrix* \mathcal{A} and *state vector* \mathcal{S} . Every *vertex* v of this graph will hold a *state* $s(v)$. The *neighborhood* $N(v)$ of a vertex is defined as the set of its adjacent vertices:

$$\mathcal{A}_{ij} = \begin{cases} 1 & \text{if } v_i \in N(v_j) \\ 0 & \text{otherwise} \end{cases} \quad \mathcal{S}_i = s(v_i) \in \{0, 1\}. \quad (1)$$

The *configuration* $c(v)$ of a vertex is a number that, when the vertices are indexed as in Figure 2, can be expressed as:

$$c(v) = 4 \times s(v) + \sum_{i \in N(v)} s(i). \quad (2)$$

The space of possible ETA rules is finite. For each of the eight configurations, a rule must specify whether the vertex will be dead or alive at $t + 1$. Consequently, there are only $2^8 = 256$ possible rules. For this reason, ETA can be seen as the two-dimensional counterpart of Wolfram's 256 elementary cellular automata [19, 20]. In fact, there is a direct equivalence between 64 of each (see Section 2.5). Furthermore, the triangle is the regular polygon tiling two-dimensional space with the smallest number of neighbors per cell. ETA are thus the most basic two-dimensional cellular automata and have a fundamental aspect in this regard.

Each *rule* R is a map from *configuration* space to *state* space:

$$R : \{0, 1, 2, 3, 4, 5, 6, 7\} \rightarrow \{0, 1\} \quad (3)$$

$$R(c_t(v)) = s_{t+1}(v).$$

Each rule can be labeled by a unique *rule number* n :

$$n = \sum_{i=0}^7 2^i R(i). \quad (4)$$

We use the labeling system that was independently proposed in [8] and [18], since it must be somewhat natural and because it has useful properties. This system, inspired by the Wolfram code [19], is such that a rule number in its binary form displays the behavior of the rule. Starting from the right, its digits indicate the future state for each configuration as they have been ordered previously. Figure 4 shows the example of rule 210.

● **Author Query:**

Figure 4 (and other similar images) scale funny. I used Magnification to fit the margin.

Is the source code available?

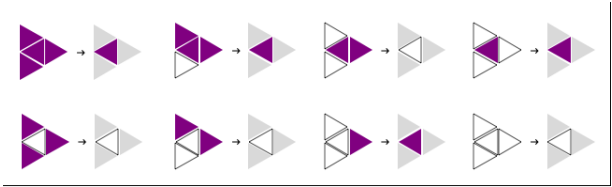


Figure 4. Rule 210 = 1101, 0010₂.

2. Behavior

Before going into the details of how to compute these automata, we can take a look at how they behave. In this section, a preliminary study of ETA is presented to motivate a future, more in-depth analysis. It is of particular interest to see what happens to a single living cell under different ETA rules so, unless otherwise noted, the following figures come from this starting point.

2.1 Beauty

One of the most striking aspects of these automata is their aesthetic quality, which cannot be better illustrated than by a few selected examples shown in Figure 5.

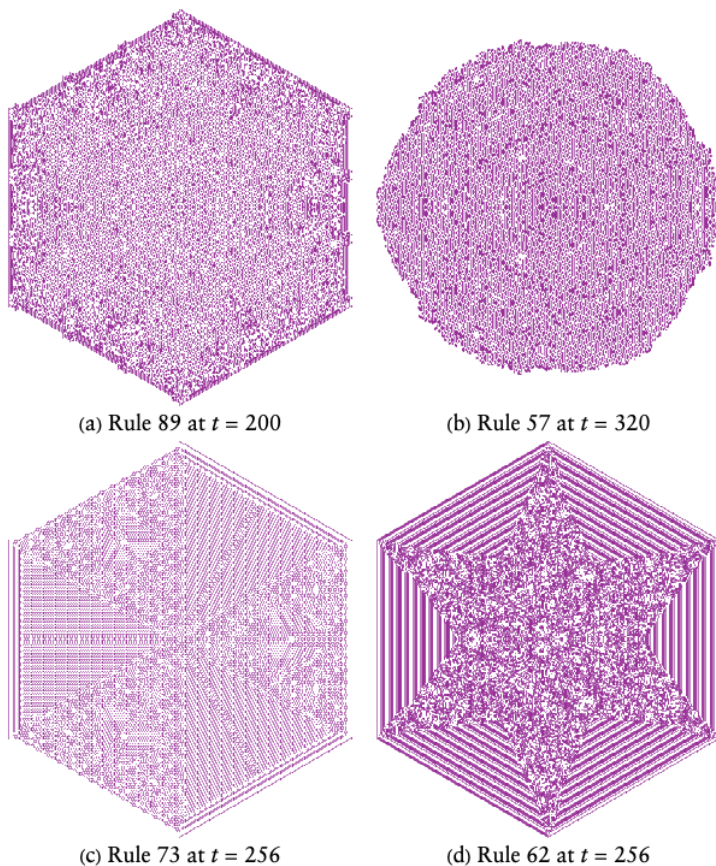
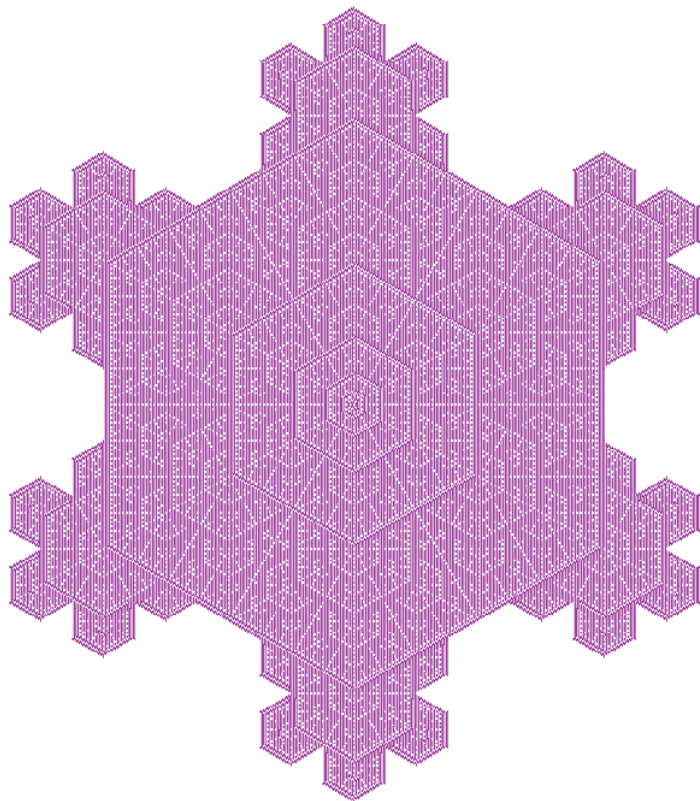


Figure 5. The beauty of ETA. (a) Rule 89 at $t = 200$. (b) Rule 57 at $t = 320$. (c) Rule 73 at $t = 256$. (d) Rule 62 at $t = 256$.

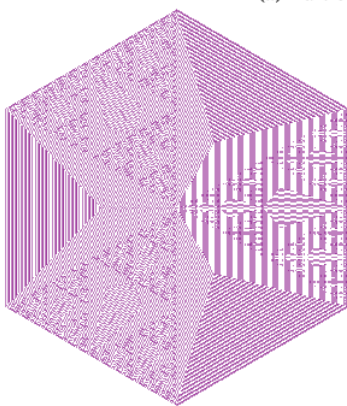
2.2 Chaos

Given the existing literature on cellular automata, it is quite expected to see some of these rules behave chaotically (Figure 6). The example of rule 53 confirms it. Starting from two randomly generated 64-layers-wide grids that are completely similar except for the central cell, which is alive in (1) and dead in (2), the trajectories strongly diverge as shown in Figure 7.

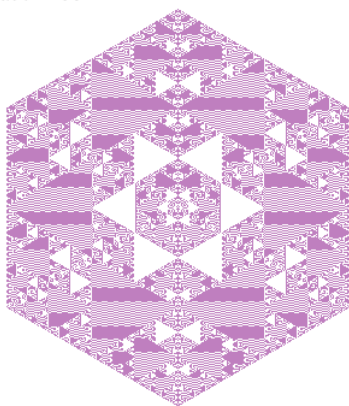
- **Author Query:**
Check Figure 6 & 7 text discussion.
Is Figure 6 caption okay as edited?



(a) Rule 50 at $t = 352$



(b) Rule 65 at $t = 512$



(c) Rule 106 at $t = 510$

Figure 6. Behavior of (a) rule 50 at $t = 352$, (b) rule 65 at $t = 512$, (c) rule 106 at $t = 510$.

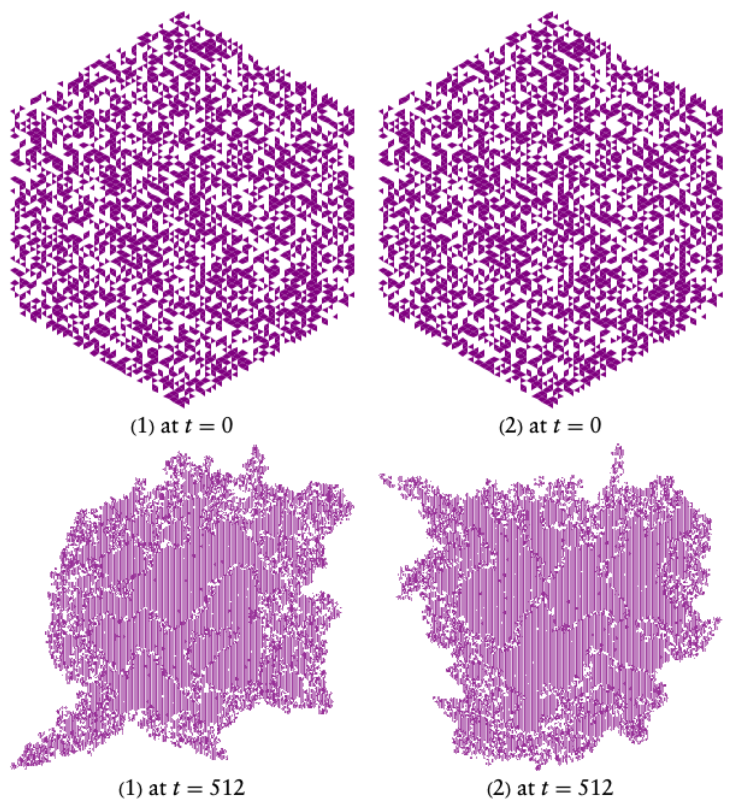


Figure 7. Chaotic behavior of rule 53.

2.3 Fractals

Some ETA rules produce remarkable scale-free structures, as shown in Figure 8.

● **Author Query:**
Is source code for Figure 8 available?

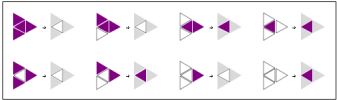


Figure 8. (a) Rule 65 at $t = 512$. (b) Rule 106 at $t = 510$. (c) Rule 50 at $t = 352$.

2.4 Spacetime

Similar to the way elementary cellular automata [19, 20] are most often represented, the evolution of an ETA can be displayed in one single plot. Here, an instant is two dimensional, so adding the dimension of time creates a three-dimensional structure. In these *spacetime plots*, time flows downward. The successive grids are stacked beneath each other, starting from the initial conditions at the top. To avoid the infinite planes created by an alive environment, we can display only the cells that have the opposite state to it at each time step. A lot of information is therefore lost. We do not see most of the internal structure and we cannot know the state of the environment. Nevertheless, this representation helps visualize some properties of ETA that are difficult to notice otherwise. For instance, certain rules create three-dimensional spacetime fractals, as seen in Figure 9.

● **Author Query:**

rephrase the preceding, meaning unclear:

To avoid the infinite planes created by an alive environment, we can display only the cells that have the opposite state to it at each time step.

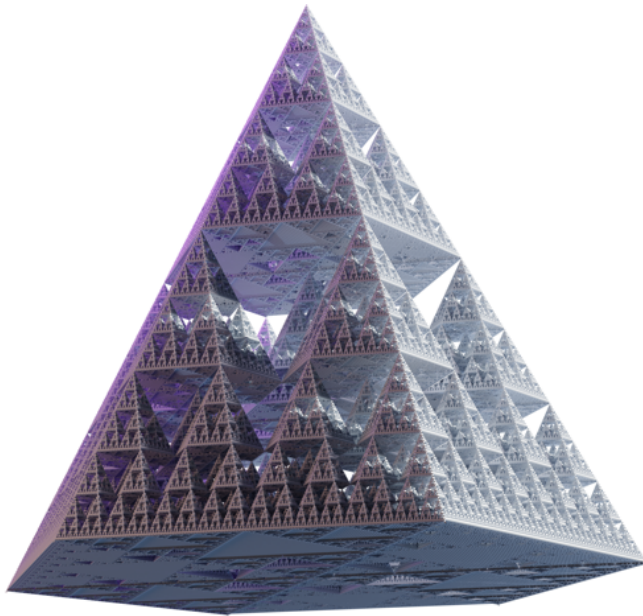


Figure 9. Spacetime plot of rule 10 up to $t = 512$.

Another way to see the time evolution of an ETA in a single plot is to look at just one line of the grid, that is, to look at a sliced space-time plot from the side (Figure 10). There is a most natural way to slice: along the lines that preserve the neighborhood relations.

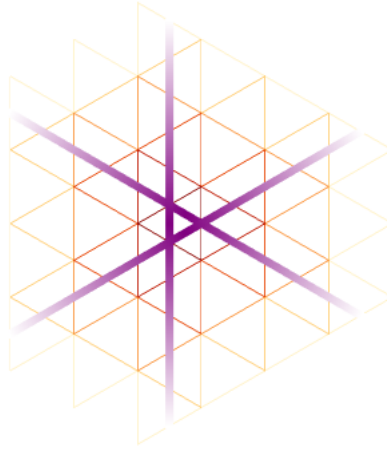


Figure 10. Natural slicing lines.

The states along these lines can be plotted beneath each other to create Wolfram-style plots, here called *slice plots* (Figure 11).

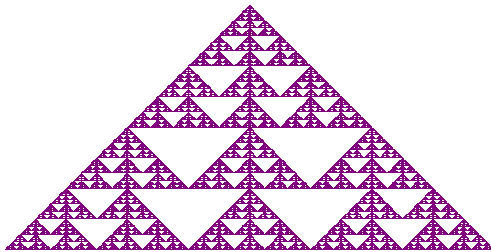


Figure 11. Slice plot of rule 10 up to $t = 512$.

2.5 Elementary Cellular Automata

Under a certain condition, ETA rules maintain the uniformity of layers. This is the case when the second and third digits of the binary rule number are the same, as well as the sixth and seventh:

$$[R(1) = R(2)] \wedge [R(5) = R(6)]. \quad (5)$$

64 ETA rules satisfy this condition, and they are all strictly equivalent to a unique symmetric elementary cellular automaton [19]; see Figure 12.

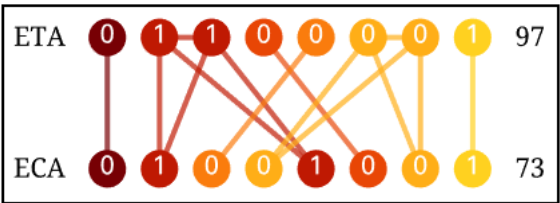


Figure 12. Conversion between ETA and elementary cellular automaton rules.

In this case, taking a slice plot (Figure 13) of the ETA gives the classic elementary cellular automaton plot (Figure 14).

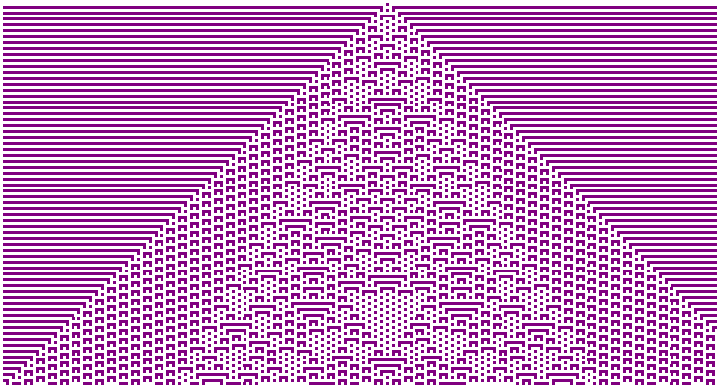


Figure 13. Slice plot of rule 97 (elementary cellular automaton rule 73) up to $t = 128$.

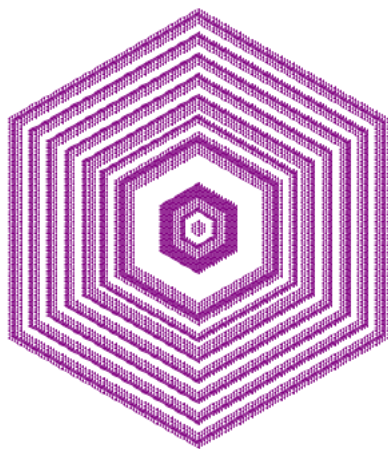


Figure 14. Rule 97 at $t = 128$.

2.6 Center Column

There are a few rules where the state of the first living cell evolves in an interesting way. This sequence of states forms the center column of the spacetime plots seen in Figure 15.

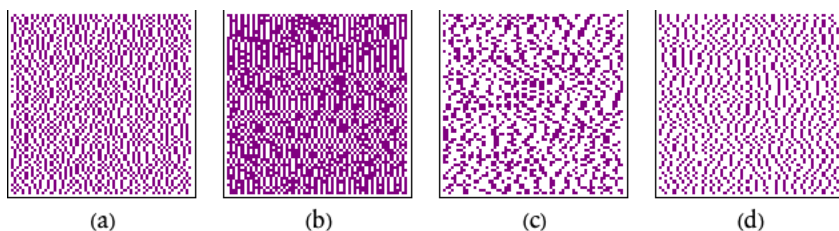


Figure 15. Center columns $1 \leq t \leq 4096$ (read left-to-right). (a) Rule 37 (OEIS A371844). (b) Rule 61 (OEIS A372553). (c) Rule 62 (OEIS A371931). (d) Rule 94 (OEIS A372552).

The symmetries of the triangle impose that, starting from a single living cell, layers 1 and 2 remain uniform. We therefore have a three-layer-wide pillar, which is fully described by a sequence of bit triplets. These can be mapped to RGB colors to extend the previous plots (Figure 16).

● **Author Query:**
Redice fotn size slightly.

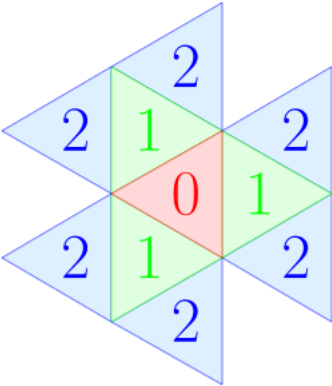


Figure 16. RGB map.



Figure 17. Living cells with corresponding colors.

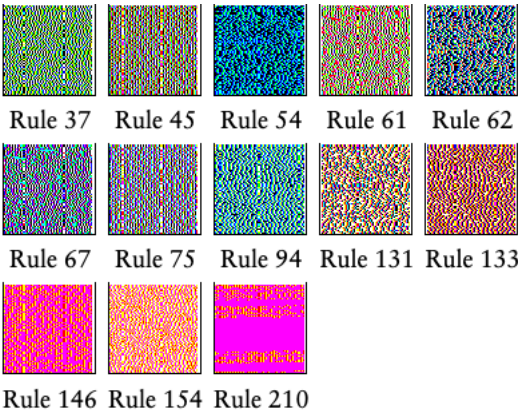


Figure 18. Three center columns $1 \leq t \leq 4096$.

2.7 Self-Reproduction

As mentioned in [17], one of the original motivations for the development of cellular automata was to create a mathematical model of self-reproduction. Interestingly, four of the 256 ETA rules naturally reproduce any finite pattern given as initial conditions: rules 85, 90, 165 and 170. A proof of self-reproduction based on path counting already exists for rule 170 [17]. Similar proofs could probably be proposed for the others.

<i>t</i>	rule 85	rule 90	rule 165	rule 170
0				
16				
32				
48				
112				

Table 1. Pattern self-reproduction from a recognizable starting point.

■ 2.8 Rule 210

Rule 210 is easy to describe: “change the state of cells that have one neighbor alive.” It is special for several reasons: it creates larger structures as time goes on and a new type of structure appears from around $t = 1024$, as shown in Figures 19–22.

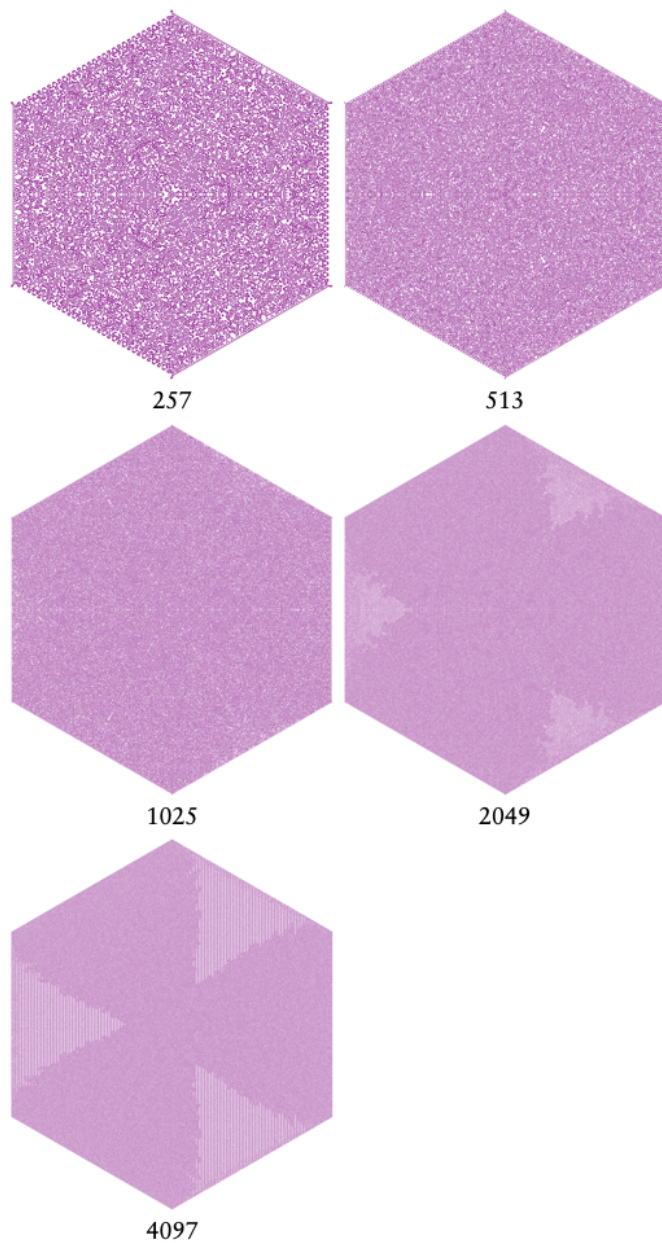


Figure 19. Rule 210 at $t = 2^i + 1$ (the structure is best seen on odd time steps from afar).

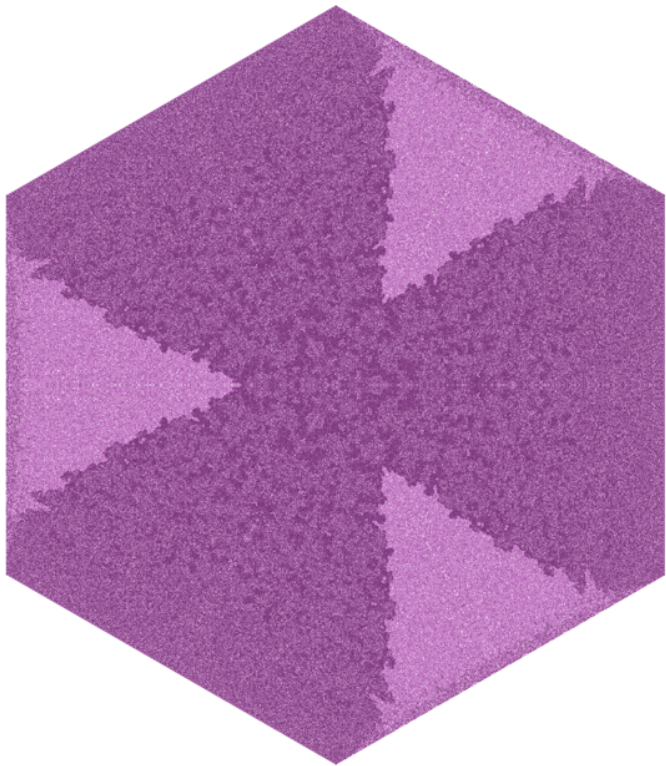


Figure 20. Rule 210 at $t = 4097$ with enhanced contrast.

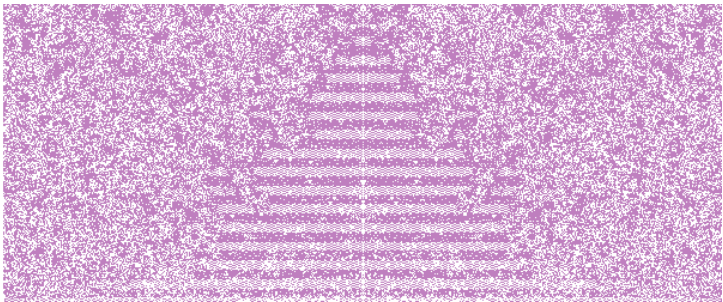


Figure 21. Close-up of rule 210 at $t = 2048$.

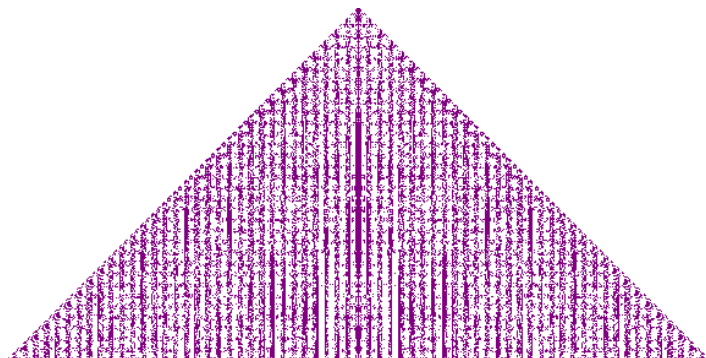


Figure 22. Slice plot of rule 210 up to $t = 4096$.

Rule 210 initially alternates between what seems like two population densities (i.e., number of living cells/size of the first cell's region of influence). When the new structure appears, around $t = 1024$, the population stabilizes in a density cycle of period 4 between slowly evolving values (Figure 23).

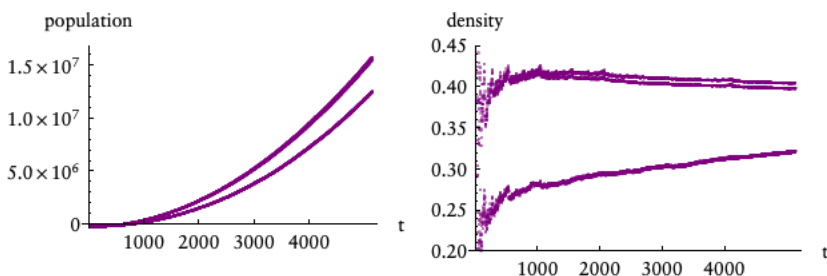


Figure 23. Evolution of two coarse-grained values under rule 210. (a) Population (OEIS A372581). (b) Population density.

2.9 Noise

Some rules seem to generate a pretty good amount of noise. For example, if we pick a simple starting point without symmetries (Figure 24), rule 37 will usually turn it into an expanding disk with a random-looking interior, as shown in Figure 25.



Figure 24. Simple asymmetric starting point.

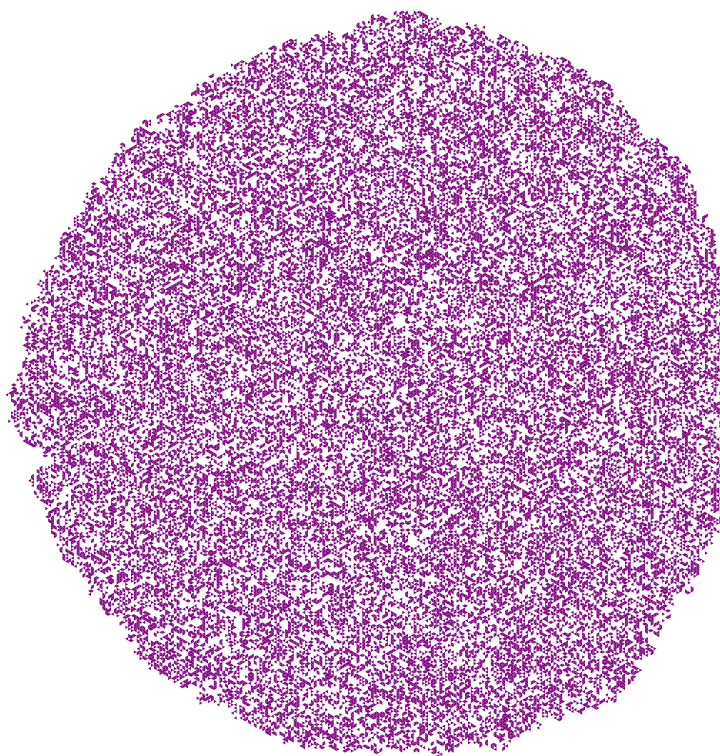


Figure 25. Result at $t = 512$ with rule 37.

2.10 Textures

Organic textures can be obtained by applying other rules to the pseudorandom grid in Figure 25, as shown in Figure 26.

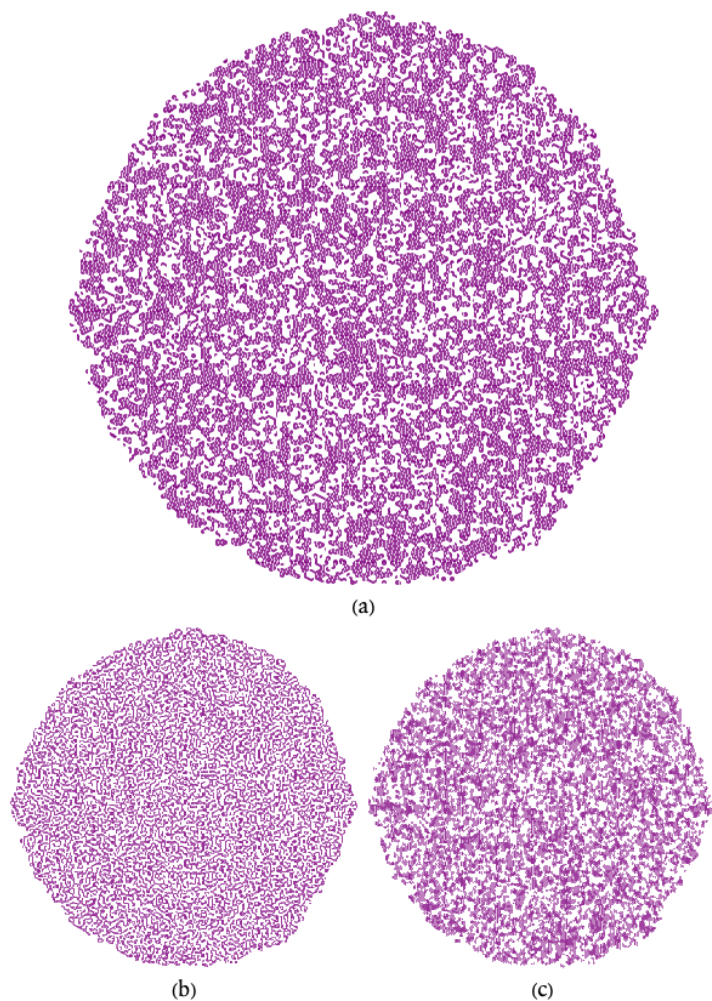


Figure 26. Starting from Figure 25. (a) Rule 204 at $t = 32$. (b) Rule 100 at $t = 64$. (c) Rule 108 at $t = 512$.

2.11 Boring Rules

There is an *identity* rule which leaves any grid unchanged: rule 240 (Figure 27).

- **Author Query:**
Is source code for Figures 27 and 28 available?

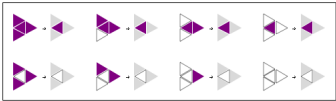


Figure 27. Rule 240.

And a *negative* rule that swaps alive and dead states: rule 15 (Figure 28).

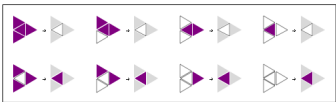
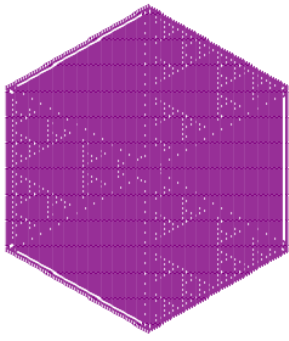


Figure 28. Rule 15.

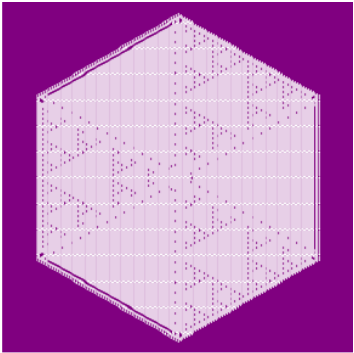
2.12 Twins

A simple procedure can be followed to find the evil twin of a rule that has the same effect but in the negative world. To find it, take the number in its binary form (with the leading zeros needed for the number to be eight digits long), swap ones and zeros and read it backward. Let us take rule 214 as an example (Figure 29).

First, find the binary form of the rule number, $214 = 11\ 010\ 110_2$
then swap ones and zeros $00\ 101\ 001_2$
and finally reverse it. $10\ 010\ 100_2 = 148$



(a)



(b)

Figure 29. Twin rules. (a) Rule 214 from one living cell at $t = 128$. (b) Rule 148 from one dead cell at $t = 128$.

3. Implementation

3.1 Tools

1. \diamond here represents an operator that joins matrices corner to corner:

$$(a) \diamond \begin{pmatrix} b & c \\ d & e \end{pmatrix} \diamond (f \quad g \quad h) = \begin{pmatrix} a & 0 & 0 & 0 & 0 & 0 \\ 0 & b & c & 0 & 0 & 0 \\ 0 & d & e & 0 & 0 & 0 \\ 0 & 0 & 0 & f & g & h \end{pmatrix} \quad (6)$$

2. \succ shifts diagonally the elements of a matrix and places the last row and column first:

$$\begin{pmatrix} a & b & c & d \\ e & f & g & h \\ i & j & k & l \end{pmatrix} \succ \begin{pmatrix} l & i & j & k \\ d & a & b & c \\ h & e & f & g \end{pmatrix} \quad (7)$$

3. $@$ will be an operator applying a function to every element of a matrix:

$$f @ \begin{pmatrix} a & b \\ c & d \end{pmatrix} = \begin{pmatrix} f(a) & f(b) \\ f(c) & f(d) \end{pmatrix} \quad (8)$$

4. \mathbb{I}_i is the $i \times i$ identity matrix. \mathbb{S}_i will be a $i \times (i + 1)$ “stairs” matrix:

$$\mathbb{I}_1 = (1) \quad \mathbb{I}_2 = \begin{pmatrix} 1 & 0 \\ 0 & 1 \end{pmatrix} \\ \mathbb{I}_3 = \begin{pmatrix} 1 & 0 & 0 \\ 0 & 1 & 0 \\ 0 & 0 & 1 \end{pmatrix} \quad \dots \quad (9)$$

$$\mathbb{S}_1 = (1 \quad 1) \quad \mathbb{S}_2 = \begin{pmatrix} 1 & 1 & 0 \\ 0 & 1 & 1 \end{pmatrix} \\ \mathbb{S}_3 = \begin{pmatrix} 1 & 1 & 0 & 0 \\ 0 & 1 & 1 & 0 \\ 0 & 0 & 1 & 1 \end{pmatrix} \quad \dots \quad (10)$$

3.2 Growing the Triangular Grid

As mentioned in Section 1, the grid will be grown from a single cell by adding layers. The cells will be ordered counterclockwise, with the first vertex of each new layer placed on the southeast diagonal (see Figure 30).

● **Author Query:**

Reduce font size slightly, can you outline the faintest numbers?

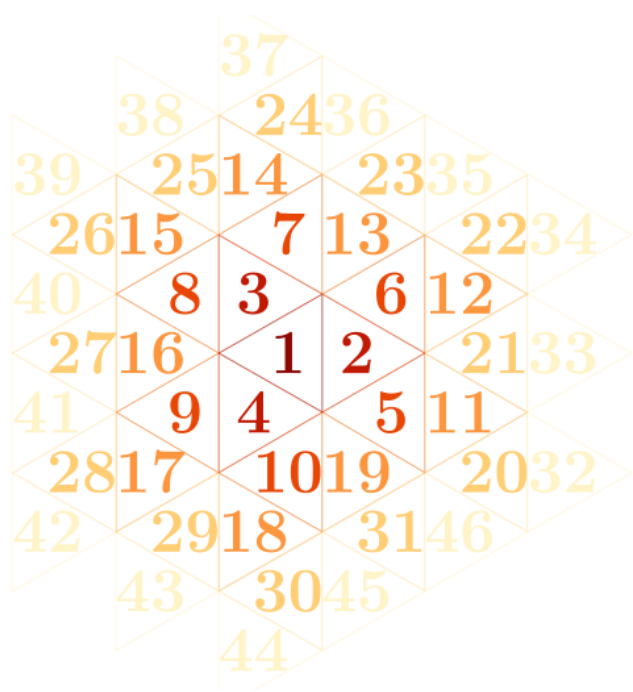


Figure 30. Cell ordering.

This is done with a precursor of the adjacency matrix called the *grid matrix* \mathcal{G} . Up to the third layer, the grid matrix is better hand-coded. The third matrix \mathcal{G}_3 can be seen in Figure 31. The subsequent layers will follow a repeating pattern.

● Author Query:

Color not available. Can the “layers” be grouped together instead?

$$\begin{pmatrix} 0 & 1 & 1 & 1 & 0 & 0 & 0 & 0 & 0 & 0 & 0 & 0 & 0 & 0 & 0 & 0 & 0 & 0 \\ 0 & 0 & 0 & 0 & 1 & 1 & 0 & 0 & 0 & 0 & 0 & 0 & 0 & 0 & 0 & 0 & 0 & 0 \\ 0 & 0 & 0 & 0 & 0 & 0 & 1 & 1 & 0 & 0 & 0 & 0 & 0 & 0 & 0 & 0 & 0 & 0 \\ 0 & 0 & 0 & 0 & 0 & 0 & 0 & 0 & 1 & 1 & 0 & 0 & 0 & 0 & 0 & 0 & 0 & 0 \\ 0 & 0 & 0 & 0 & 0 & 0 & 0 & 0 & 0 & 0 & 1 & 0 & 0 & 0 & 0 & 0 & 0 & 1 \\ 0 & 0 & 0 & 0 & 0 & 0 & 0 & 0 & 0 & 0 & 0 & 1 & 1 & 0 & 0 & 0 & 0 & 0 \\ 0 & 0 & 0 & 0 & 0 & 0 & 0 & 0 & 0 & 0 & 0 & 0 & 1 & 1 & 0 & 0 & 0 & 0 \\ 0 & 0 & 0 & 0 & 0 & 0 & 0 & 0 & 0 & 0 & 0 & 0 & 0 & 0 & 1 & 1 & 0 & 0 \\ 0 & 0 & 0 & 0 & 0 & 0 & 0 & 0 & 0 & 0 & 0 & 0 & 0 & 0 & 0 & 1 & 1 & 0 \\ 0 & 0 & 0 & 0 & 0 & 0 & 0 & 0 & 0 & 0 & 0 & 0 & 0 & 0 & 0 & 0 & 1 & 1 \end{pmatrix}$$

Figure 31. Grid matrix \mathcal{G}_3 (with layers purple 1, red 2 and orange 3).

Each layer consists of a submatrix, and the grid matrix will be:

$$\mathcal{G}_l = m_1 \diamond m_2 \diamond \dots \diamond m_{l-1} \diamond m_l. \quad (11)$$

From m_4 , these submatrices become:

$$m_i = \begin{cases} \mathbb{S}_{\frac{i}{2}} \diamond \mathbb{I}_{\left(\frac{i}{2}-1\right)} \diamond \mathbb{S}_{\frac{i}{2}} \diamond \mathbb{I}_{\left(\frac{i}{2}-1\right)} \diamond \mathbb{S}_{\frac{i}{2}} \diamond \mathbb{I}_{\left(\frac{i}{2}-1\right)} & \text{if } i \text{ is even} \\ \left(\mathbb{I}_{\left\lceil \frac{i}{2}-2 \right\rceil} \diamond \mathbb{S}_{\left\lceil \frac{i}{2} \right\rceil} \diamond \mathbb{I}_{\left\lceil \frac{i}{2}-2 \right\rceil} \diamond \mathbb{S}_{\left\lceil \frac{i}{2} \right\rceil} \diamond \mathbb{I}_{\left\lceil \frac{i}{2}-2 \right\rceil} \diamond \mathbb{S}_{\left\lceil \frac{i}{2} \right\rceil} \right)^\vee & \text{if } i \text{ is odd.} \end{cases} \quad (12)$$

Assuming that \mathbb{I}_0 is a 0×0 matrix, this pattern actually holds for m_2 and m_3 . However, depending on how this is implemented, coding the first three layers by hand might be the best option.

Once the grid matrix is built, it is easy to obtain the adjacency matrix by turning it into a symmetric matrix as illustrated in Figure 32.

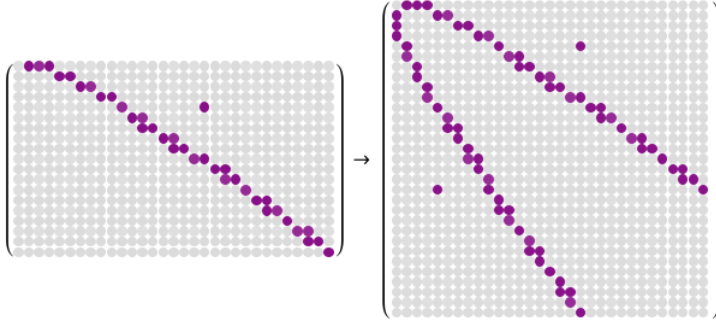


Figure 31. From the grid matrix \mathcal{G} to the adjacency matrix \mathcal{A} .

The limit of this series of matrices \mathcal{A}_∞ is the adjacency matrix of the graph corresponding to the infinite triangular grid.

3.3 Evolving the State

The environment will be simulated by using two layers around the region of the influence of our initial structure. If the initial structure is a single triangle, then the computed grid will contain $t + 2$ layers.

Updating the state of the grid will come in four steps.

1. A layer is added with the same state as the last vertex (both the grid/adjacency matrix and the state vector must be updated).
2. A *configuration vector* C is computed (o is the order of the graph):

$$C = \begin{pmatrix} c(v_1) \\ \vdots \\ c(v_o) \end{pmatrix} = 4 \times S + \mathcal{A} \cdot S. \quad (13)$$

3. The state vector S is then updated:
- $$S = R @ C. \quad (14)$$
4. The state of all vertices of the last layer (created in step 1) is set to the value of the last vertex of the now penultimate layer. This removes the artifacts coming from the edges of the computed grid.

Remarks

- Evolving the state of the grid is where this framework pays off the most. Steps 2 and 3 are mathematically sufficient if we consider working in an infinite graph. They would also be the only steps required in a closed grid, like a triangulated surface [8], for example.
- For this process to be efficient, it is necessary to encode the grid/adjacency matrix in a sparse array format.

- Step 1 can be avoided in the case where the three outermost layers have a uniform state, which is easy to check.
- It is useful here to be able to retrieve the number of layers l in the graph from its order o and vice versa:

$$\begin{aligned} l &= \frac{1}{6}(\sqrt{3(8o-5)} - 3) \\ o &= 1 + \frac{3}{2}l(l+1). \end{aligned} \quad (15)$$

- It is also useful to note that each layer l contains $3l$ vertices or cells (except when $l = 0$).

3.4 Plotting the Result

Two-dimensional coordinates are required to plot the resulting grid. These can be computed in a *coordinates matrix* \mathcal{K} . Algorithm 1 can be used to expand \mathcal{K} from the coordinates of the first vertex, placed at the origin $(0 \ 0)$:

$$\mathcal{K} = \begin{pmatrix} x_1 & y_1 \\ x_2 & y_2 \\ x_3 & y_3 \\ \vdots & \vdots \\ x_{o-2} & y_{o-2} \\ x_{o-1} & y_{o-1} \\ x_o & y_o \end{pmatrix}. \quad (16)$$

These coordinates will serve to translate a base triangle whose orientation depends on the layer it is in, as shown in Table 2.



Layer	Coordinates of the base triangle			Illustration
even	$\left(-\frac{1}{\sqrt{3}} \ 0\right)$	$\left(\frac{1}{2\sqrt{3}} \ \frac{1}{2}\right)$	$\left(\frac{1}{2\sqrt{3}} \ -\frac{1}{2}\right)$	
odd	$\left(\frac{1}{\sqrt{3}} \ 0\right)$	$\left(-\frac{1}{2\sqrt{3}} \ \frac{1}{2}\right)$	$\left(-\frac{1}{2\sqrt{3}} \ -\frac{1}{2}\right)$	

Table 2. Coordinates of the base triangle's vertices.

1. if l is odd then l is the number of the new layer
2. $\text{step} \leftarrow \left(-\frac{1}{\sqrt{3}} \ 0\right)$
3. else
4. $\text{step} \leftarrow \left(-\frac{1}{2\sqrt{3}} \ -\frac{1}{2}\right)$
5. end if

6. $\mathcal{K}.\text{append}(\mathcal{K}[-3(l-1)] + \text{step}) \quad \mathcal{K}[-n] \equiv n^{\text{th}}$ coordinates from the end
7. **for** $i \rightarrow 0, 3l-2$ **do**
8. **if** $i < \lfloor \frac{l}{2} \rfloor$ **then** $\text{step} \rightarrow (0 \quad 1)$
9. **else if** $i < \lfloor \frac{l}{2} \rfloor + \lfloor \frac{l}{2} \rfloor$ **then** $\text{step} \leftarrow \begin{pmatrix} -\frac{\sqrt{3}}{2} & \frac{1}{2} \end{pmatrix}$
10. **else if** $i < 2\lfloor \frac{l}{2} \rfloor + \lfloor \frac{l}{2} \rfloor$ **then** $\text{step} \leftarrow \begin{pmatrix} -\frac{\sqrt{3}}{2} & -\frac{1}{2} \end{pmatrix}$
11. **else if** $i < 2\lfloor \frac{l}{2} \rfloor + 2\lfloor \frac{l}{2} \rfloor$ **then** $\text{step} \leftarrow (0 \quad -1)$
12. **else if** $i < 3\lfloor \frac{l}{2} \rfloor + 2\lfloor \frac{l}{2} \rfloor$ **then** $\text{step} \leftarrow \begin{pmatrix} \frac{\sqrt{3}}{2} & -\frac{1}{2} \end{pmatrix}$
13. **else if** $i < 3\lfloor \frac{l}{2} \rfloor + 3\lfloor \frac{l}{2} \rfloor$ **then** $\text{step} \leftarrow \begin{pmatrix} \frac{\sqrt{3}}{2} & \frac{1}{2} \end{pmatrix}$
14. **end if**
15. $\mathcal{K}.\text{append}(\mathcal{K}[-1] + \text{step})$
16. **end for**

Algorithm 1. Adding a layer to the coordinates matrix \mathcal{K} .

4. Conclusion

The triangular tessellation plays an important role in many disciplines, from computer graphics to architecture. Triangular automata (TA) are a way of populating the triangular tessellation space with aesthetic patterns. Beyond the possible applications, elementary triangular automata (ETA) are somewhat fundamental cellular automata, making them an elegant model of complexity. With the framework presented here, the 256 ETA rules can now be thoroughly explored, even with limited computational resources.

Here are some possible directions for future work:

1. ETA rules could be classified according to some common criteria.
2. The approach taken in this paper could easily be applied to a wider class of TA.
3. A GPU-accelerated implementation could be used to explore longer timescales, as has already been done for graph-rewriting automata [21].
4. Turing completeness and other interesting properties could be searched for in ETA rules.

References

- [1] R. W. Gerling, “Classification of Triangular and Honeycomb Cellular Automata,” *Physica A: Statistical Mechanics and Its Applications*, 162(2), 1990 pp. 196–209. doi:10.1016/0378-4371(90)90438-X.
- [2] C. Bays, “Cellular Automata in the Triangular Tessellation,” *Complex Systems*, 8(2), 1994 pp. 127–150. complex-systems.com/pdf/08-2-4.pdf.

- [3] K. Imai and K. Morita, “A Computation-Universal Two-Dimensional 8-State Triangular Reversible Cellular Automaton,” *Theoretical Computer Science*, **231**(2), 2000 pp. 181–191. doi:10.1016/S0304-3975(99)00099-7.
- [4] L. Naumov, “Generalized Coordinates for Cellular Automata Grids,” in *Computational Science—ICCS 2003: International Conference Proceedings, Part II*, Melbourne, Australia and St. Petersburg, Russia (P. M. A. Sloot, D. Abramson, A. V. Bogdanov, Y. E. Gorbachev, J. J. Dongarra and A. Y. Zomaya, eds.), Berlin, Heidelberg: Springer, 2003 pp. 869–878. doi:10.1007/3-540-44862-4_94.
- [5] Y. Lin, A. Mynett and Q. Chen, “Application of Unstructured Cellular Automata on Ecological Modelling,” in *Advances in Water Resources and Hydraulic Engineering: Proceedings of 16th IAHR-APD Congress and 3rd Symposium of IAHR-ISHS*, Nanjing, China (C. Zhang and H. Tang, eds.), Berlin, Heidelberg: Springer 2009 pp. 624–629. doi:10.1007/978-3-540-89465-0_108.
- [6] C. Bays, “Cellular Automata in Triangular, Pentagonal and Hexagonal Tessellations,” *Encyclopedia of Complexity and Systems Science* (R. Meyers, ed.), New York: Springer, 2009 pp. 892–900.
- [7] C. Bays, “The Game of Life in Non-square Environments,” *Game of Life Cellular Automata* (A. Adamatzky, ed.), New York: Springer, 2010 pp. 319–329. doi:10.1007/978-1-84996-217-9_17.
- [8] M. Zawidzki, “Application of Semitotalistic 2D Cellular Automata on a Triangulated 3D Surface,” *International Journal of Design & Nature and Ecodynamics*, **6**(1), 2011 pp. 34–51. doi:10.2495/DNE-V6-N1-34-51.
- [9] B. Breckling, G. Pe’er and Y. G. Matsinos, “Cellular Automata in Ecological Modelling,” *Modelling Complex Ecological Dynamics: An Introduction into Ecological Modelling for Students, Teachers & Scientists* (F. Jopp, H. Reuter and B. Breckling eds.), Berlin, Heidelberg: Springer, 2011 pp. 105–117. doi:10.1007/978-3-642-05029-9_8.
- [10] M. Saadat, “Cellular Automata in the Triangular Grid,” Master’s thesis, Eastern Mediterranean University (EMU)-Doğu Akdeniz Üniversitesi (DAÜ), 2016.
- [11] G. M. Ortigoza, A. Lorandi and I. Neri, “ACFUEGOS: An Unstructured Triangular Cellular Automata for Modelling Forest Fire Propagation,” in *High Performance Computer Applications (ISUM 2015)*, Mexico City, Mexico (I. Gitler and J. Klapp, eds.), Cham: Springer International Publishing, 2016 pp. 132–143. doi:10.1007/978-3-319-32243-8_9.
- [12] S. Uguz, S. Redjepov, E. Acar and H. Akin, “Structure and Reversibility of 2D von Neumann Cellular Automata over Triangular Lattice,” *International Journal of Bifurcation and Chaos*, **27**(6), 2017 1750083. doi:10.1142/S0218127417500833.

- [13] M. Saadat and B. Nagy, “Cellular Automata Approach to Mathematical Morphology in the Triangular Grid,” *Acta Polytechnica Hungarica*, 15(6), 2018 pp. 45–62. doi:10.12700/APH.15.6.2018.6.3.
- [14] G. A. Wainer, “An Introduction to Cellular Automata Models with Cell-DEVS,” in *2019 Winter Simulation Conference (WSC’19)*, National Harbor, MD, Piscataway, NJ: IEEE, 2019 pp. 1534–1548. doi:10.1109/WSC40007.2019.9004763.
- [15] A. V. Pavlova, S. E. Rubtsov and I. S. Telyatnikov, “Using Cellular Automata in Modelling of the Fire Front Propagation through Rough Terrain,” *IOP Conference Series: Earth and Environmental Science*, 579(1), 2020 012104. doi:10.1088/1755-1315/579/1/012104.
- [16] M. R. Saadat and B. Nagy, “Generating Patterns on the Triangular Grid by Cellular Automata including Alternating Use of Two Rules,” in *2021 12th International Symposium on Image and Signal Processing and Analysis (ISPA’21)*, Zagreb, Croatia (T. Petkovic, D. Petrinovic and S. Loncaric, eds.), Piscataway, NJ: IEEE, 2021 pp. 253–258. doi:10.1109/ISPA52656.2021.9552107.
- [17] M. R. Saadat and B. Nagy, “Copy Machines—Self-reproduction with 2 States on Archimedean Tilings,” *Journal of Cellular Automata*, 17(3–4), 2023 pp. 221–249.
- [18] P. Cousin and A. Maignan, “Organic Structures Emerging from Bio-Inspired Graph-Rewriting Automata,” in *2022 24th International Symposium on Symbolic and Numeric Algorithms for Scientific Computing (SYNASC)*, Hagenberg/Linz, Austria (B. Buchberger, M. Marin, V. Negru and D. Zaharie, eds.), Piscataway, NJ: IEEE, 2022, pp. 293–296. doi:10.1109/SYNASC57785.2022.00053.
- [19] S. Wolfram, *A New Kind of Science*, Champaign, IL: Wolfram Media, Inc., 2002.
- [20] E. W. Weisstein. “Elementary Cellular Automaton” from MathWorld—A Wolfram Web Resource. (Aug 29, 2024) mathworld.wolfram.com/ElementaryCellularAutomaton.html.
- [21] P. Cousin. “Graph-Rewriting Automata.” (Aug 29, 2024) paulcousin.github.io/graph-rewriting-automata.